OFFICE OF NAVAL RESEARCH

GRANT: N00014-90-J-1230

R&T CODE 4133015

ROBERT J. NOWAK

Technical Report No. 63

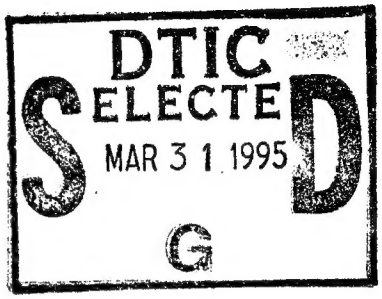

Electron Transfer Kinetics of Self-assembled Ferrocen C(12) Alkanethiol Monolayers on Gold Electrodes from 125K to 175K

by

John N. Richardson, Gary K. Rowe, Michael T. Carter, Leonard M. Tender, Larry S. Curtin, Stephen R. Peak and Royce W. Murray

Prepared for Publication

in the

Electrochimica Acta

University of North Carolina at Chapel Hill
Department of Chemistry
Chapel Hill, NC

March 1, 1995

REPORT DOCUMENTATION PAGE

Form Approved
OMB No. 0704-0188

1. AGENCY USE ONLY (Leave blank)	2. REPORT DATE	3. REPORT TYPE AND DATES COVERED
	March 23, 1995	Interim

4. TITLE AND SUBTITLE

Electron Transfer Kinetics of Self-Assembled Ferrocene C(12) Alkanethiol Monolayers on Gold Electrodes from 125K to 175K

5. FUNDING NUMBERS

N00014-90-J-1230

6. AUTHOR(S)

John N. Richardson, Gary K. Rowe, Michael T. Carter, Leonard M. Tender, Larry S. Curtin, Stephen R. Peak and Royce W. Murray

7. PERFORMING ORGANIZATION NAME(S) AND ADDRESS(ES)

The University of North Carolina at Chapel Hill
Department of Chemistry
Chapel Hill, N.C. 27599-3290

8. PERFORMING ORGANIZATION REPORT NUMBER

63

9. SPONSORING/MONITORING AGENCY NAME(S) AND ADDRESS(ES)

Office of Naval Research
Department of the Navy
Arlington, VA 22217

10. SPONSORING/MONITORING AGENCY REPORT NUMBER

11. SUPPLEMENTARY NOTES

12a. DISTRIBUTION/AVAILABILITY STATEMENT

Approved for Public Release, Distribution Unlimited

12b. DISTRIBUTION CODE

13. ABSTRACT (Maximum 200 words)

The electron transfer kinetics of monolayers of $CpFeCpCO_2(CH_2)_{12}SH$ and $CH_3(CH_2)_{11}SH$ co-chemisorbed on gold electrodes have been measured in 2:1 (v:v) chloroethane/butyronitrile solvent at temperatures ranging from 125K to 175K with potential steps and cyclic voltammetry. Rate constants, k°, measured using cyclic voltammetry range from $3x10^{-4}$ to 10^{-1} s^{-1} over these temperatures; an activation plot of $\log[k^o/k_bT^{1/2}]$ *vs.* 1/T gave $\lambda = 0.89$ eV for the reorganization energy for the $Cp_2Fe^{+/0}$ reaction and a pre-factor of $6.5x10^6$ $eV^{-1}s^{-1}$. The rate constants were obtained by comparison of experimental ΔE_{PEAK} values with those of cyclic voltammograms digitally simulated with Marcus-DOS theory. A value of $\lambda = 0.76$ eV is predicted from dielectric continuum theory. The $CpFeCpCO_2(CH_2)_{12}SH$ monolayers are kinetically inhomogeneous (disperse) as shown by non-linear ln[i] *vs.* time plots in potential step experiments. The kinetic dispersity has adverse effects on determinations of λ values from cyclic voltammetric waveshapes and from plots of potential step-derived rate constants, $k_{app,\eta}$, against overpotential (η), producing depressed values for λ.

14. SUBJECT TERMS

Ferrocene, Electron-transfer kinetics, Monolayers

15. NUMBER OF PAGES

32

16. PRICE CODE

17. SECURITY CLASSIFICATION OF REPORT	18. SECURITY CLASSIFICATION OF THIS PAGE	19. SECURITY CLASSIFICATION OF ABSTRACT	20. LIMITATION OF ABSTRACT
Unclassified	Unclassified	Unclassified	Unlimited

October 12, 1994

ELECTRON TRANSFER KINETICS OF SELF-ASSEMBLED FERROCENE (C12)ALKANETHIOL MONOLAYERS ON GOLD ELECTRODES FROM 125K to 175K

John N. Richardson, Gary K. Rowe, Michael T. Carter, Leonard M. Tender[1], Larry S. Curtin[2], Stephen R. Peck[3], and Royce W. Murray*

Kenan Laboratories of Chemistry, University of North Carolina at Chapel Hill, Chapel Hill, NC 27599-3290

ABSTRACT

The electron transfer kinetics of monolayers of $CpFeCpCO_2(CH_2)_{12}SH$ and $CH_3(CH_2)_{11}SH$ co-chemisorbed on gold electrodes have been measured in 2:1 (v:v) chloroethane/butyronitrile solvent at temperatures ranging from 125K to 175K with potential steps and cyclic voltammetry. Rate constants, k°, measured using cyclic voltammetry range from $3x10^{-4}$ to 10^{-1} s^{-1} over these temperatures; an activation plot of $\log[k^\circ/k_bT^{1/2}]$ *vs.* $1/T$ gave λ = 0.89 eV for the reorganization energy for the $Cp_2Fe^{+/0}$ reaction and a pre-factor of $6.5x10^6$ $eV^{-1}s^{-1}$. The rate constants were obtained by comparison of experimental ΔE_{PEAK} values with those of cyclic voltammograms digitally simulated with Marcus-DOS theory. A value of λ = 0.76 eV is predicted from dielectric continuum theory. The $CpFeCpCO_2(CH_2)_{12}SH$ monolayers are kinetically inhomogeneous (disperse) as shown by non-linear ln[i] *vs.* time plots in potential step experiments. The kinetic dispersity has adverse effects on determinations of λ values from cyclic voltammetric waveshapes and from plots of potential step-derived rate constants, $k_{app,\eta}$, against overpotential (η), producing depressed values for λ.

[1]present address: Department of Chemistry, Stanford University, Stanford, CA 94305

[2]present address: Department of Chemistry, Temple University, Philadelphia, PA 19122

[3]present address: E. I. DuPont de Nemours & Co. (Inc), P. O. Box 1217, Parkersburg, WV 26102

Keywords: Electrode kinetics, self-assembled monolayers, low temperature, ferrocene, reorganization energy

ELECTRON TRANSFER KINETICS OF SELF-ASSEMBLED FERROCENE (C12)ALKANETHIOL MONOLAYERS ON GOLD ELECTRODES FROM 125K to 175K

Molecular monolayers organized by hydrophobic forces are long-standing objects of research in chemistry and molecular biology. In recent years, the combining[1] of hydrophobic forces and surface chemisorption has opened new avenues for fabrication and study of molecular films. In particular, chemisorption and self-assembly of alkanethiols and their derivatives on metal surfaces, notably gold, is undergoing detailed scrutiny in investigations of chemically modified electrode interfaces[2] and of the dynamics of electron transfers between the electrode and reactants positioned on the solution side of an organized alkane monolayer barrier.[3] There have been important corollary studies on mixed monolayers[4] and monolayer structure[5], and related investigations of chemically modified metal surface wetting[6], corrosion[7], and patterning[8]. Measurements of electrode kinetics at self-assembled monolayers[3] promise to provide important new insights into how the detailed molecular environment of an electrode reactant affects its reactivity[1b], and into the chemistry of electron tunneling[9]. Control of the distance between electrode reactants and electrode was a long-standing goal in research on chemically modified electrodes[10], and has become a recent target in design of interfaces for study of electron transfer dynamics at superconducting electrodes.[3f]

This paper will describe measurements of low temperature electron transfer kinetics in self-assembled mixed monolayers of ferrocene ester dodecanethiol, $CpFeCpCO_2(CH_2)_{12}SH$, and dodecanethiol, $CH_3(CH_2)_{11}SH$. The $Cp_2Fe^{+/0}$ electrode reaction is studied in a binary cryoelectrochemical solvent[11], 2:1 (v:v)

chloroethane:butyronitrile (EtCl/PrCN) over a temperature range of 125K to 175K, measuring its standard electron transfer rate constant k° using cyclic voltammetric and potential step experiments. We have previously shown[2m] that $CpFeCpCO_2(CH_2)_{12}SH$ and shorter chain $CpFeCp(CH_2)_8SH$ monolayers are exceptionally stable in this low temperature medium. Experiments on the electrode kinetics of $CpFeCp(CH_2)_8SH$ and of $CpFeCpCO_2(CH_2)_8SH$ monolayers on Au and Ag electrodes are described elsewhere.[3g] Central questions in the present study have been the suitability of various approaches to measurement of k° and of the reorganization energy λ, and whether these parameters exhibit any unusual properties as a result of the lowered temperatures or of the organic solvent medium. These questions are inter-connected because, in contrast to those described by Chidsey et al[3a], the ferrocene ester alkanethiol monolayers studied here are not kinetically homogeneous, probably in part due to the organic solvent environment. The kinetic inhomogeneity has adverse consequences on the suitability of different measurement approaches to λ.

EXPERIMENTAL

Chemicals. Ferrocene ester dodecanethiol, $CpFeCpCO_2(CH_2)_{12}SH$ (Cp = cyclopentadienyl) was prepared by a literature method.[4a] Dodecanethiol ($CH_3(CH_2)_{11}SH$, Aldrich 97%), butyronitrile (Aldrich, 99+ %), absolute ethanol (AAPER Alcohol and Chemical Co.), and tetra-n-butylammonium hexafluorophosphate supporting electrolyte (Bu_4NPF_6, Fluka, Puriss) were used as received. Chloroethane (Linde) was condensed and stored in sealed vacuum transfer pipets at room temperature. Water was purified (>18 Mohm/cm^2) with a Barnstead NANO pure system.

Electrode Fabrication and Preparation. Working and reference electrodes were 0.5 mm and 2.0 mm diameter gold rods (Johnson Matthey Electronics, 99.999 %), respectively, encapsulated in and exposed at the end of an epoxy cylinder (Shell Epon 828, *m*-phenylenediamine curing agent, cured overnight at 70° C). The metal disks were polished before each experiment with 1μm alumina (Buehler) and 1 μm diamond paste (Buehler) with extensive rinsing with water and sonication. Prior to immersion in the thiol coating solution, the gold surfaces were etched in dilute *aqua regia* for five minutes[12] and thoroughly rinsed with water and ethanol.

Chemisorbed Monolayer Preparation. Coating solutions consisted of a 1:3 (**M:M**) ratio of $CpFeCpCO_2(CH_2)_{12}SH$ and $CH_3(CH_2)_{11}SH$ in ethanol at 1mM total thiol concentration. The $CH_3(CH_2)_{11}SH$ diluent thiol is employed to minimize lateral interactions between the ferrocene sites[4a]. The etched electrodes were exposed to this solution for >24 hours, thoroughly rinsed with ethanol, and dried. The Au pseudo-reference electrode was scraped to expose a fresh Au surface. Annealing-incubation of chemisorbed films in fresh diluent solution was not employed.[4a]

Electrochemical Measurements. The cylindrical electrode assembly was fitted into a slotted stainless steel sleeve whose Pt bottom served as an auxiliary electrode spaced *ca.* 0.5 mm from the working/reference electrodes. The electrodes were placed in an aluminum container containing the desired quantity of butyronitrile and Bu_4NPF_6 (0.075M final concentration), pre-chilled to dry ice temperature to avoid thiol desorption. The cell was sealed, immersed in a dry ice/acetone slush bath, evacuated, and chloroethane was vacuum transferred to the final solution volume. The cell was bolted to the cold finger of a Janis

helium refrigerator cryostat interfaced to a Lakeshore Cryogenics 320 Autotuning Temperature Controller, and brought to the desired temperature, which required *ca.* 4 hour. Further temperature changes of ≤10° required *ca.* 1 hour for equilibration.

Cyclic voltammetric and potential step experiments were executed with instruments of local design, employing A/D conversion and digital data storage, low-pass filtering of analog signals during slow timescale, and positive feedback iR compensation to counter the low solution ionic conductivities. The latter step was particularly important given that, for example, without feedback, the potentiostatically uncompensated resistance between working and reference electrodes at 125K was as large as 550kΩ. (Uncompensated solution resistances were measured by AC impedance with a Schlumberger-Solartron Instruments Model 1255 frequency response analyzer and Model 1286 potentiostat.) Positive feedback in cyclic voltammetry and potential step experiments was implemented by incrementally increasing the proportionality constant between cell current and feedback potential added to the applied electrode potential until the circuit became slightly unstable (current oscillation), then backing off to restore circuit stability. We have found that such instrumental correction for resistance effects is well-suited to low temperature work in which the measured currents are small and experimental time scales long.

Potential step experiments were initiated from the formal potential ($E^{o'}$, determined by cyclic voltammetry) of the $Cp_2Fe^{+/0}$ couple; the applied overpotentials varied from ±30 mV to ±500 mV. Corrections for background currents, which were minor, were obtained from potential steps in the double-layer potential region negative of $E^{o'}$. Coverages of electroactive ferrocene (Γ) were measured from the charge under slow potential scan

(10mV/s) cyclic voltammograms.

RESULTS AND DISCUSSION

Measurements of Heterogeneous Electron Transfer Rate Constants With Cyclic Voltammetry. Typical examples of low temperature cyclic voltammograms of mixed $CpFeCpCO_2(CH_2)_{12}SH/CH_3(CH_2)_{11}SH$ monolayers are shown in Figure 1. The voltammograms are well-defined, show symmetrical oxidation/reduction branches, and are extremely stable, remaining unchanged over hours of potential cycling at these temperatures. The quantities of ferrocene sites present in the monolayers are governed by the ferrocene/diluent ratio in the coating solutions; typical ferrocene coverages (Figure 1) are *ca.* 1/4 to 1/3 of a full monolayer.[4a,13]

Figure 1 shows that the separation ΔE_{PEAK} between oxidation and reduction peak potentials in $CpFeCpCO_2(CH_2)_{12}SH$ monolayer voltammetry increases as the electron transfer rate is thermally quenched by lowered temperatures. ΔE_{PEAK} also increases at increased potential sweep rate as shown in Table I.

From theory by Laviron[14] based on the Butler-Volmer formalism for electrode kinetics[15], ΔE_{PEAK} is governed by the electron transfer rate constant of the surface-attached redox species. Laviron theory has been employed by others[3c,4a] to evaluate electrode kinetics from cyclic voltammograms of self-assembled electroactive monolayers. We have chosen to employ a Marcus theory formulation[16,17] to evaluate rate constants from ΔE_{PEAK} results since Marcus theory is more appropriate when the reaction overpotential is not negligible in comparison to its reorganization energy, λ. The pertinent equation is[3a,3c]

$$k_{red,ox} = \mu \rho k_b T \int_{-\infty}^{\infty} \frac{\exp[-(x-\frac{\lambda \pm \eta}{k_b T})^2 \frac{k_b T}{4\lambda}]}{1+\exp(x)} dx \qquad (1)$$

where μ is the electronic coupling (tunneling) parameter, ρ the density of electronic states in the metal electrode, k_b the Boltzmann constant, T the Kelvin temperature, and η the applied overpotential. This equation contains an integration of the electronic states around the Fermi level; we refer[17a] to it as Marcus-DOS theory. Equation 1 has been used[17] in digital simulations of cyclic voltammograms to examine the relationships between theoretical waveshapes and ΔE_{PEAK} values ($\Delta E_{PEAK}/2 = \eta$), and reaction and experimental parameters such as the rate constant k^o, λ, T, and potential sweep rate, v. An example of a theoretical working plot of ΔE_{PEAK} *vs.* $\log(v/k^o)$, calculated for 125K, is given in Figure 2 as is an analogous plot based on Butler Volmer theory (for $\alpha = 0.5$).

Figure 2 shows that, firstly, ΔE_{PEAK} values predicted by Marcus theory are, except when ΔE_{PEAK} is relatively small, substantially larger than those predicted by standard Butler Volmer theory. The consequence is that rate constants evaluated when ΔE_{PEAK} is large with the latter electrode kinetic model would tend to be too small[17a]. Secondly, especially for larger λ, ΔE_{PEAK} values are relatively insensitive to its value (although waveshape and peak current are strongly sensitive to λ, *vide infra*). This characteristic[17a] of ΔE_{PEAK} insensitivity to λ is beneficial in that k^o can be estimated reliably from ΔE_{PEAK} without accurate prior knowledge of λ. For example, in the present work an experimental cyclic voltammogram for a $CpFeCpCO_2(CH_2)_{12}SH$ monolayer at 130K and 50 mV/s gave a ΔE_{PEAK} = 410 mV; comparing this result to versions of Figure 2 calculated for 130K and λ = 0.6 *vs.* 1.0 eV

produces k^o = 0.0009 *vs.* 0.00063 s^{-1}, respectively, a variation of only *ca.* 50% for these two assumptions of λ.

ΔE_{PEAK} values determined as a function of potential sweep rate at different temperatures for $CpFeCpCO_2(CH_2)_{12}SH$ monolayers are compared to theoretical working curves in Figure 3. The theoretical curves were calculated for λ = 0.7 eV. The figure shows that at each temperature it is possible to select a rate constant that produces a good fit between the theoretical curve and the sweep rate data. Table I gives results of point-by-point calculations of k^o, again using λ = 0.7 eV working curves.[18] Besides the temperature dependency of the rate constant k^o, the most significant aspect of Table I is that k^o does not vary with v, in particular k^o does not trend downward with increasing v. A potential sweep rate dependency of measured rate constants is generally symptomatic of bias of ΔE_{PEAK} values caused by iR_{UNC} problems; its absence here is taken as evidence that the resistance compensation technique employed (see Experimental) satisfactorily avoids such problems in cyclic voltammetry. In addition, estimation of iR_{UNC} from the product of voltammetric peak currents and directly measured R_{UNC} (see Table I footnote) gives voltages which are small relative to the measured ΔE_{PEAK} values, even before positive feedback compensation is applied. Table II gives k^o values, averaged over different sweep rates, for a larger variety of temperatures.

The variation of the cyclic voltammetrically measured k^o with temperature was analyzed for the reorganization energy λ by the activation relation

$$k^o = \mu\rho k_b T \exp\left(-\frac{\Delta G^*}{k_b T}\right) \qquad (2)$$

where ΔG^{*} the free energy of activation is $\lambda/4$ (assuming on the basis of literature data[20] a negligible entropy of activation). Analysis of the Table II k°_{CV} results as a plot[19] of $\ln(k^{\circ}/k_b T^{1/2})$ *vs.* 1/T reveals a linear activation plot (Figure 4(□)) with slope corresponding to a 0.89 eV reorganization energy.

The result of Figure 4(□) can be compared to the dielectric continuum model[16] for barrier control by the energetics of solvent dipole (outer sphere) reorganization, which is

$$\lambda = \frac{e^2 N}{8\pi\epsilon_o}\left(\frac{1}{a}-\frac{1}{2d}\right)\left(\frac{1}{\epsilon_{op}}-\frac{1}{\epsilon_s}\right) \qquad (3)$$

where e is the electronic charge, N Avogadro's number, ϵ_o the permittivity of free space, a the reactant radius and d its separation from the electrode surface, and ϵ_{op} and ϵ_s the optical and static dielectric constants, respectively. Several assumptions are involved here: (*i*) Reactions of ferrocene species are generally thought to be mainly outer sphere barrier-controlled[20], which is assumed here. (*ii*) d is 18.7×10^{-10} m based on an all *trans* 30° tilted alkane chain configuration[4a] and treating the ester linkages as equivalent to two additional methylene units.[21] (*iii*) The small, linear temperature dependencies[22,23] of ϵ_{op} and ϵ_s for EtCl and PrCN have been extrapolated to our range of temperatures[24] and combined as an "average" dielectric continuum with "average" dielectric properties ϵ_{op} and ϵ_s that are sums of the mole-fraction-weighted individual constants. The sensitivity of λ to temperature is very small (predicted λ is 0.78 eV at 293K and 0.76 eV at 175K), and since the more important ϵ_{op} term is similar for EtCl and PrCN, an averaged dielectric seems reasonable.

(*iv*) The ferrocene is actually positioned at a high polarity (EtCl/PrCN)-low polarity (the alkane chains) interface, whereas our use of Equation 3 assumes uniform solvation by the high polarity medium. An analysis[25] of solvent spatial correlation effects may be a preferred approach. That Equation 3 is a simplification of the actual situation has also been noted by previous workers[3a,3c].

Irrespective of the assumptions noted above, the reorganization energy λ = 0.89 eV derived from the activation plot in Figure 4(□) is only slightly larger than the 0.76 eV prediction of Equation 3. For reasons described below, there are difficulties in other approaches to measuring λ, namely voltammetric waveshape analysis and potential step experiments, that may produce less reliable results for ionically resistive solutions and kinetically disperse monolayers.

Extrapolation of the Figure 4(□) activation plot gives a predicted room temperature k_{273}° = 36 s^{-1} and a product $\mu\rho$ = 6.5x10^6 $eV^{-1}s^{-1}$. The room temperature rate constant is not actually measureable in the EtCl/PrCN solvent since the self-assembled monolayers are stable in it only at low temperatures. The data can, however, be compared to room-temperature k^e results in aqueous acid by Chidsey[3a,3b] of *ca.* 40 s^{-1} and 2.1x10^6 $eV^{-1}s^{-1}$ for k^e and $\mu\rho$, respectively. The agreement between the k^e and $\mu\rho$ values, considering the difference in medium and the kinetic dispersion (*vide infra*) of the present monolayers, is quite reasonable.

As noted above, we have shown[17a] that cyclic voltammetric waveshapes are in Marcus-DOS theory quite sensitive to the value of reorganization energy λ. Waveshapes become broadened when λ is not much larger than $\Delta E_{PEAK}/2$. The waveshape sensitivity

can, however, be employed to measure λ *only* when the experimental voltammetry does not also experience broadening from other sources, such as a distribution of formal potentials ($E^{o'}$) or of the actual rate constants among the surface redox site population. We refer to these surface population inhomogeneity effects, collectively, as kinetic dispersion[25]. The presence of kinetic dispersion will cause a λ value derived from a Marcus-DOS waveshape analysis to be erroneously small, as was demonstrated in a recent comparison[17a] of voltammetry from one $CpFeCpCO_2(CH_2)_{16}SH$ monolayer which did not exhibit kinetic dispersion (as established by linear ln[i] *vs.* time plots in potential step experiments[3a]) with a different monolayer sample which by the same criterion was kinetically disperse. This comparison[17a] also gave the important result that the rate constants k^o obtained from the kinetically homogeneous and kinetically disperse monolayers by use of working plots such as Figure 2 were in good agreement. This agreement suggests that the averaging involved in determining a rate constant with Figure 2 does not significantly bias the result towards the faster or the slower reacting sites among the ferrocene surface population. Calculations[26b] are also consistent with the experimental observation[17a], indicating only a two-fold, nearly temperature independent upward bias in a cyclic voltammetric k^o measurement of a kinetically disperse monolayer.

All ferrocene alkanethiol monolayers that we have examined[2m,3f,3g,17a] in the low temperature EtCl/PrCN solvent exhibit substantial broadening of cyclic voltammetric waveshapes and (*vide infra*) non-linear ln[i] *vs.* time plots in potential step experiments. The kinetic dispersity of these monolayers occurs probably in part by intercalation of the organic solvent into the monolayer. Figure 5 shows a comparison of waveshapes for voltammetry of

$CpFeCpCO_2(CH_2)_{12}SH$ monolayers at different temperatures, to waveshape calculations based on Marcus-DOS theory (Equation 1). It is clearly possible to select theoretical parameters that produce reasonable fits to the experimental results, and the rate constants obtained, k^o = 0.0018, 0.014, 0.09 s^{-1} at 130, 150, and 170K, are not very different from those obtained using Figure 3 with the ΔE_{PEAK} values of these voltammograms, 0.0008, 0.011, and 0.088 s^{-1}, respectively. However, the reorganization energies, λ = 0.29, 0.29, and 0.18 eV at 130, 150, and 170K, respectively, that are required to fit the theoretical waveshapes to the experimental ones are very low. These latter reorganization energy results are believed to be unreliable and are presented solely to illustrate a pitfall of kinetic dispersion.

Measurement Using Potential Steps. Chidsey[3a] and Finklea[3c] have measured heterogeneous electron transfer rate constants in electroactive self-assembled monolayers using current-time transients produced by potential steps to various overpotentials. Electrolysis of the monolayer is, ideally, a first order process, giving a current transient described by the relation

$$i_{\eta,t} = k_{app} Q \exp(-k_{app,\eta} t) \qquad (4)$$

where $k_{app,\eta}$ the sum of the forward and reverse electron transfer rate constants at overpotential η ($E_{APPLIED}$ - $E^{o'}$) is given by the slope of a ln[i] *vs.* time plot, and Q is the total charge passed in the electron transfer reaction. The linearity of such a plot of Equation 4 is an indicator that the reacting surface population is kinetically homogeneous.[3a,3c]

Figure 6 shows ln[i] *vs.* time plots acquired at 140K by stepping from $E^{o'}$ by +300,

+150, and +70 mV, using positive feedback iR compensation[27]. Immediately obvious are the substantial differences in current and time-scale as η is varied, and that the plots exhibit curvature toward smaller slope at all overpotentials. The latter effect is symptomatic of a kinetically disperse or non-uniform monolayer. We have analyzed these dispersive kinetics by dividing the current-time transient into segments of charge passed, which serves to define the different, sequentially reacting, populations of surface ferrocene sites. The vertical lines on Figure 6 indicate, for example, the beginning and end of passage of charges which are the 0.5 to 0.8 fraction of the total reaction charge ($nFA[\Gamma]/2$). The plots' slopes during passage of each such increment of charge (or of any smaller increment) represents the kinetics of that particular segment of the reacting surface population. The rate constants of such population segments can then be compared as to their dependency on the applied overpotential.

Figure 7 plots rate constants $k_{APP,\eta}$ for the successive 0.5 to 0.6, 0.6 to 0.7, and 0.7 to 0.8 charge-based segments of reacting population in experiments in which the size of the potential step (η) was varied, and for experiments at several temperatures. These results show that the variation of rate constants for the three charge segments (the three over-lapping data points at each η and temperature) is, while noticeable, small in comparison of the variations of rate constant due to changes in η or in temperature. We see that the rate constants in Figure 7 do not follow the exponential increase with overpotential classically expected from Butler Volmer theory, but instead fold over at higher η as anticipated by Marcus-DOS theory[3a,3c] when η is not negligible with respect to reorganization energy λ. It is further significant that, like results[3a] for kinetically uniform ferrocene monolayers in

aqueous acid, the variation in rate constant with η is symmetrical about $\eta = 0$. As discussed by Finklea[3c] such symmetry is evidence for a through-bond tunneling mechanism.

Over-lying each of the sets of $\log[k_{APP,\eta N}]$ *vs.* η data in Figure 7 are best fit curves(——) derived by comparison of Equation 1 to the data. Table II contains the values of k° and λ corresponding to the fits in Figure 7 and for further experiments. Examining these results, we see firstly that rate constants derived from the potential step analysis are in generally good agreement (within a factor of two) with those obtained (*vide supra*) from cyclic voltammetry. Secondly, the reorganization energy obtained from the $\log[k_{APP,\eta}]$ *vs.* η fits of Equation 1 at the highest temperature, 0.80 eV at 150K, is close to that obtained, 0.89 eV, from the activation analysis of the k°_{CV} data (Figure 4(○)). Unexpected, however, is the apparent temperature dependence of λ of the reorganization energy, in which we see λ decrease to 0.46 eV at the lowest temperature. Thirdly, the pre-factor $\mu\rho$ of Equation 1 obtained in the fitting is at 150K, $5.3\text{x}10^5$ $eV^{-1}s^{-1}$. This $\mu\rho$ value can be compared to data by Chidsey[3b] which gives $\mu\rho = 2.1\text{x}10^6$ $eV^{-1}s^{-1}$ for $CpFeCpCO_2(CH_2)_{12}SH$ monolayers in aqueous $HClO_4$ at 273K. Fourthly, below 150K, consistent with the changes seen in λ, the values of $\mu\rho$ (not shown) corresponding to the Table II data become much smaller, falling to $4.2\text{x}10^2$ $eV^{-1}s^{-1}$ at 125K. As explained next, we believe the λ results at the lower temperatures (shown parenthetically in Table II) are not reliable.

The rate constants for the 0.5 to 0.8 population segments were selected for analysis in Figure 7 since these data are potentially less distorted by residual uncompensated resistances than those collected during earlier reacting segments where the currents are larger. One consequence of a resistance effect, if present, would be to depress k_{APP} values

obtained at larger η (where higher currents flow) more than those obtained at lower η; the added curvature thus induced in $\log[k_{APP}]$ *vs.* η plots would consequently depress the result for λ. This error would be most serious at lower temperatures since ionic conductivities decrease with decreasing temperature. (We do not on the other hand believe that resistance effects are a problem in the cyclic voltammetric experiments due to both the results of Table I and because the currents passed in those experiments are much smaller than in Figure 6.)

Even were resistance effects absent in the potential step experiments, kinetic dispersity in the monolayers can cause spurious results in data analyses like Figure 7. As described elsewhere[26b], simulation of the effects of a spread in ferrocene formal potentials $E^{o\prime}$ on a potential step rate measurement, shows that the $E^{o\prime}$ dispersion causes (*i*) *curved* ln[i] *vs.* time plots, and (*ii*) depressed values for k^{o}, λ, and $\mu\rho$ upon analysis with Equation 1, for all charge segments and especially early ones. We are as a consequence skeptical of the parenthetically shown potential step results in Table II for λ.

The k^{o} results from potential step experiments are plotted according to Equation 3 in Figure 4(O), and give from the slope λ = 0.66 eV. This value of the reorganization energy is smaller than that obtained, 0.89 eV, from the cyclic voltammetric data, Figure 4(□) and slightly smaller than predicted by theory, 0.76 eV. The k^{o} values determined in potential step experiments (and the λ values derived from them) are apparently somewhat less affected by the problem noted above.

In summary, the resistive low temperature environment and the kinetic dispersion in the $CpFeCpCO_2(CH_2)_{12}SH$ monolayers present a challenging measurement situation within

which are pitfalls that we believe can lead to distortions in the kinetic results. The derivation of rate constants k^o from analysis of cyclic voltammetric ΔE_{PEAK} results and of λ by activation plots of those rate constants appear to be most immune to such distortions.

ACKNOWLEDGEMENT. This research was funded in part by grants from the Office of Naval Research and the National Science Foundation.

REFERENCES

1. (a) A. Ulman, *An Introduction To Ultra-thin Organic Films From Langmuir Blodgett to Self-assembly*; Academic Press: San Diego, (1991). (b) A. J. Bard, H. D. Abruna, C. E. D. Chidsey, L. R. Faulkner, S. Feldberg, K. Itaya, M. M. Majda, O. Melroy, R. W. Murray, M. Porter, M. Soriaga, H. S. White, *J. Phys. Chem.*, 97, 7147 (1993).

2. (a) C. A. Goss, C. J. Miller, M. Majda, *J. Phys. Chem. 92*, 1937 (1988). (b) I. Rubinstein, S. Steinberg, Y. Tor, A. Shanzer, *Nature 332*, 426 (1988). (c) S. E. Creager, G. K. Rowe, *Anal. Chem. Acta 246*, 233 (1991). (d) H. C. De Long, J. J. Donohue, D. A. Buttry, *Langmuir 7*, 2196 (1991). (e) R. V. Duevel, R. M. Corn, *Anal. Chem. 64*, 337 (1992). (f) H. Sellers, A. Ulman, Y. Shnidman, J. E. Eilers, *J. Amer. Chem. Soc. 115*, 9389 (1993). (g) K. A. Groat, S. E. Creager, *Langmuir 9*, 3668 (1993). (h) J. J. Hickman, P. E. Laibinis, D. I. Auerbach, C. Zou, T. J. Gardner, G. M. Whitesides, M. S. Wrighton, *Langmuir 8*, 357 (1992). (i) M. D. Porter, T. B. Bright, D. L. Allara, C. E. D. Chidsey, *J. Amer. Chem. Soc. 109*, 3559 (1987). (j) H.

O. Finklea, D. A. Snider, J. Fedyk, *Langmuir 6*, 371 (1990). (k) H. O. Finklea, D. D. Hanshew, *J. Electroanal. Chem. 347*, 327 (1993). (l) J. Redepenning, H. M. Tunison, H. O. Finklea, *Langmuir 9*, 1404 (1993). (m) L. S. Curtin, S. R. Peck, L. M. Tender, R. W. Murray, G. K. Rowe, S. E. Creager, *Anal. Chem. 65*, 386 (1993).

3. (a) C. E. D. Chidsey, *Science 251*, 919 (1991). (b) L. H. Dubois, R. G. Nuzzo, *Annu. Rev. Phys. Chem. 43*, 437 (1992). (c) H. O. Finklea, D. D. Hanshew, *J. Amer. Chem. Soc. 114*, 3173 (1992). (d) H. O. Finklea, M. S. Ravenscroft, D. A. Snider, *Langmuir 9*, 223 (1993). (e) A. M. Becka, C. J. Miller, *J. Phys. Chem. 97*, 6233 (1993). (f) S. R. Peck, L. S. Curtin, L. M. Tender, M. T. Carter, R. H. Terrill, R. W. Murray, J. P. Collman, W. A. Little, H. M. Duan, C. Dong, A. M. Hermann, submitted for publication. (g) R. N. Richardson, S. R. Peck, L. S. Curtin, L. M. Tender, R. H. Terrill, M. Carter, R. W. Murray, G. K. Rowe, S. E. Creager, submitted for publication.

4. (a) C. E. D. Chidsey, C. R. Bertozzi, T. M. Putvinski, A. M. Mujsce, *J. Amer. Chem. Soc. 112*, 4301 (1990). (b) J. P. Folkers, P. E. Laibinis, G. M. Whitesides, J. Deutch, *J. Phys. Chem. 98*, 563 (1994). (c) S. D. Evans, P. Sanassy, A. Ulman, *Thin Solid Films 243*, 325 (1994). (d) G. K. Rowe, S. E. Creager, *Langmuir 10*, 1186 (1994).

5. (a) S. Shogen, M. Kawasaki, T. Kondo, Y. Sato, K. Uosaki, *Appl. Organomet. Chem. 6*, 533 (1992). (b) B. E. Winger, R. K. Julian, R. G. Cooks, C. E. D. Chidsey, *J. Amer. Chem. Soc. 113*, 8967 (1991). (c) S. D. Evans, T. L. Freeman, T. M. Flynn, D. N. Batchelder, A. Ulman, *Thin Solid Films 244*, 778 (1994). (d) N. Camillone, C. E. D. Chidsey, G. Y. Liu, G. Scoles, *J. Chem. Phys. 98*, 3503 (1993)

6. (a) M. K. Chaudhury, G. M. Whitesides, *Science 256*, 1539 (1992). (b) P. E. Laibinis, R. G. Nuzzo, G. M. Whitesides, *J. Phys. Chem. 96*, 5097 (1992).

7. P. E. Laibinis, G. M. Whitesides, *J. Amer. Chem. Soc. 114*, 9022 (1992).

8. A. Kumar, H. A. Biebuyck, N. L. Abbott, G. M. Whitesides, *J. Amer. Chem. Soc. 114*, 9188 (1992).

9. (a) B. Paulson, K. Pramod, P. Eaton, G. Closs, J. R. Miller, *J. Phys. Chem. 97*, 13042 (1993). (b) D. R. Casimiro, J. H. Richards, J. R. Winkler, H. Gray, *Ibid.*, 13073 (1993).

10. R. W. Murray, *Molecular Design of Electrode Surfaces*, Wiley-Interscience, N.Y. 1992.

11. S. Ching, J. T. McDevitt, S. R. Peck, R. W. Murray, *J. Electrochem. Soc. 138*, 2308 (1991).

12. S. E. Creager, L. A. Hockett, G. K. Rowe, *Langmuir 8*, 854 (1992).

13. This coverage level is a compromise between minimizing ferrocene-ferrocene interactions and obtaining adequate current signal/background ratios.

14. E. Laviron, E. *J. Electroanal. Chem.*, *101*, 19 (1979).

15. A. J. Bard, L. R. Faulkner *Electrochemical Methods*, Wiley, N.Y., 1980.

16. R. A. Marcus, *J. Chem. Phys. 43*, 679 (1965).

17. a) Tender, L. M.; Carter, M. T.; Murray, R. W. *Anal. Chem.* **1994**, *66*, 3173. b) Weber, K.; Creager, S. E. *Ibid*, pp. 3164.

18. These results would change very little if λ = 0.7±0.1eV working curves were employed.

19. (a) Equation 2 does not indicate the temperature dependence of μ

($=(H_{AB}^2/\hbar)(\pi/\lambda k_b T)^{1/2}$); a $\ln(k^o/k_b T^{1/2})$ *vs.* $1/T$ plot accounts for this dependence. Ignoring it has only minor effects; Figure 4 as a $\ln(k^o/k_b T)$ plot would give $\lambda = 0.85$ eV for the cyclic voltammetry data. b) R. A. Marcus, N. Sutin, *Biochim Biophysica Acta 811*, 265 (1985).

20. T. Gennett, D. F. Milner, M. J. Weaver *J. Phys. Chem. 89*, 2787 (1985).

21. In studies[3g] of ferrocene ester octanethiol and of ferrocene octanethiol, an 11-fold rate difference (ester being slower) is consistent with an ester linkage tunnelling barrier length equivalent to that of two methylene units.

22. J. A. Ridick, W. B. Bunder, T. K. Sahano, "Organic Solvents-Physical Properties and Methods of Purification"; John Wiley and Sons: New York, 1986.

23. O. Madelung, "Landolt-Bornstein: Numerical Data and Functional Relationships in Science and Technology: Vol 6, Static Dielectric Constants of Pure Liquids and Binary Liquid Mixtures"; Springer-Verlag: New York, 1991.

24. For example, the extrapolated ϵ_{op} and ϵ_s values for EtCl at 175K are 2.051 and 18.62; those for EtCl at 125K are 2.127 and 22.06; those for PrCN at 175K are 2.054 and 36.51; those for PrCN at 125K are 2.113 and 41.47, respectively. The weighted sums of ϵ_{op} and ϵ_s at 175K are 2.052 and 23.81 and at 125K are 2.123 and 27.69, respectively. These yield λ = 0.76 and 0.74 eV in Equation 3 at 175K and 125K, respectively.

25. D. K. Phelps, A. A. Kornyshev, M. J. Weaver *J. Phys. Chem. 94*, 1454 (1990).

26. (a) Assuming a Gaussian distribution among the $E^{o\prime}$ values of the redox sites in a monolayer can readily represent[26b] the degree of broadening of typical low

temperature voltammetric waves. Further, calculations for potential step experiments show[24b] that a spread among the thermodynamic potentials can, since applied overpotential η is referenced to the average $E^{o\prime}$, cause curved ln[i] *vs.* time plots for such experiments, thus mimicking a dispersion of rate constants among the surface redox sites. This apparent dispersion would add to any real dispersion among rate constants that might also be present. The $E^{o\prime}$-based kinetic dispersion also has a substantial effect on plots of $\log[k_{APP}]$ *vs.* η, introducing curvature at large η that in analysis of such plots by Equation 1 causes smaller apparent values of k^{o}, λ, and $\mu\rho$.

(b) G. K. Rowe, M. T. Carter, J. N. Richardson, R. W. Murray, submitted for publication.

27. The transients of Figure 6 were corrected for background currents with transients resulting from with the same magntiude potential step in the double layer region that lies negative of the surface $Cp_2Fe^{+/0}$ couple.

TABLE I. Heterogeneous electron transfer rate constants obtained from cyclic voltammetry as a function of potential sweep rate and temperature.[a]

	v, mV/s	ΔE_{PEAK}, mV	k^o, s^{-1} [b]
T=125K	5	327	0.00027
	10	361	0.00030
	20	398	0.00030
	50	452	0.00030
T=135K	5	251	0.0015
	10	290	0.0015
	20	330	0.0015
	50	383	0.0016
T=145K	5	181	0.0065
	10	220	0.0065
	20	261	0.0065
	50	312	0.0070
T=150K	5	149	0.0125
	10	188	0.0125
	20	227	0.0123
	50	286	0.0123

a) Uncompensated resistances determined using AC impedance at T = 125, 130, 135, 145, and 150K are R_{UNC} = $5.5x10^5$, $2.3x10^5$, $9.3x10^4$, $2.7x10^4$, and $1.6x10^4$ Ω, respectively. These are values before positive feedback compensation is applied. b) from comparison of experimental ΔE_{PEAK} to those of digitally simulated voltammograms, assuming λ = 0.7 eV (see text).

TABLE II. Rate parameters from analysis of $\log(k_{app})$ *vs.* η plots and cyclic voltammetry as a function of temperature.

T(K)	k^o, s^{-1} (E step)[a]	λ, eV (E step)[a]	k^o, s^{-1} (CV)[b]
125	0.0005	(0.46)	0.00029
130	0.001	(0.48)	0.0008
135	0.002	(0.49)	0.0017
140	0.003	(0.56)	0.0032
145	0.004	0.78	0.0064
150	0.008	0.80	0.012
155	---	---	0.020
160	---	---	0.034
165	---	---	0.057
170	---	---	0.090
175	---	---	0.136

a) From analysis of $\log(k_{APP,\eta})$ *vs.* η plots (see text). Activation analysis of these data gives λ = 0.66 eV, $\mu\rho$ = 7.4×10^4 $eV^{-1}s^{-1}$, and an extrapolated k_{273} = 3.2 s^{-1}, all smaller than data from CV analysis. b) from comparison of experimental ΔE_{PEAK} to those of digitally simulated voltammograms, assuming λ = 0.7 eV (see text). Activation analysis of these data gives λ = 0.89 eV and $\mu\rho$ = 6.5×10^6 $eV^{-1}s^{-1}$.

FIGURE CAPTIONS

Figure 1. Cyclic voltammograms (50 mV/s) of mixed $CpFeCpCO_2(CH_2)_{12}SH$/ $CH_3(CH_2)_{11}SH$ monolayer in 2:1 (v:v) EtCl/PrCN solvent at T = 130K (———), 150K (- - -), and 170K (——). Electroactive ferrocene coverages are $1.4x10^{-10}$, $1.5x10^{-10}$ and $1.6x10^{-10}$ mol/cm^2, respectively.

Figure 2. ΔE_{PEAK} *vs.* log(v/k°, units are volts) at 125K from digitally simulated cyclic voltammograms based on Marcus-DOS theory (Eqn. 1) as a function of reorganization energy: λ = 0.2 eV (□), 0.4 eV (▽), 0.7 eV (Δ), and 1.0 eV (+). (——) represents result using Butler-Volmer theory for α = 0.5.

Figure 3. Experimental ΔE_{PEAK} *vs.* log(v/k°, units are volts) at 130K(□) and k° = 0.0008 s^{-1}, 140K(O) and k° = 0.0032 s^{-1}, and 150K(Δ) and k° = 0.012 s^{-1}, compared to digitally simulated cyclic voltammograms at those temperatures, based on Marcus-DOS theory (Equation 1) and a reorganization energy λ = 0.7 eV.

Figure 4. Activation plot of Equation 2 for experimental k° data in Table II, from cyclic voltammograms (□) and log[$k_{APP,\eta}$] *vs.* η plots (O), slopes and intercepts give λ = 0.89 eV and 0.66 eV, and $\mu\rho$ = $6.5x10^6$ $eV^{-1}s^{-1}$, and $7.4x10^4$ $eV^{-1}s^{-1}$, respectively, were calculated from the slopes of these plots.

Figure 5. Waveshape fits of experimental (oxidation branch) voltammetric waves, v = 50 mV/s at 130K(□), 150(O), and 170K(Δ), to waveshapes calculated based on Equation 1 and k° = 0.0018 s^{-1}, λ = 0.29 eV (130K); k° = 0.014 s^{-1}, λ = 0.29 eV (150K); and k° = 0.09 s^{-1}, λ = 0.18 eV (170K).

Figure 6 ln[i] *vs.* time transients obtained at 140K at η = +300 mV (panel A), +150 mV

(panel B), and +70 mV (panel C). Vertical lines represent boundaries of the fractions 0.5 to 0.8 of the total charge passed in the reaction, $nFA\Gamma/2$. The average $k_{app,\eta}$ over this charge segment is 30, 0.63, and 0.036 s^{-1} for the 300, 150, and 70 mV potential steps, respectively.

Figure 7. (O) Oxidation and reduction branches of a 140K composite $\log(k_{APP,\eta})$ *vs.* η plot (Tafel plot) constructed using $k_{APP,\eta}$ values from 0.5-0.6, 0.6-0.7 and 0.7-0.8 charge segments (bottom-to-top of three O shown) of total reacting charge in the step; (□) same but 130K and oxidation branch only; (Δ) same but 150K and oxidation branch only; (——) are best fit lines from Equation 1 for parameters (130K) k° = 0.001 s^{-1}, λ = 0.48 eV, and $\mu\rho$ = 8.2×10^2 $eV^{-1}s^{-1}$, (140K) k° = 0.0025s^{-1}, λ = 0.52 eV, and $\mu\rho$ = 2.0×10^3 $eV^{-1}s^{-1}$, and (150K) k° = 0.008 s^{-1}, λ = 0.80 eV, and $\mu\rho$ = 5.3×10^5 $eV^{-1}s^{-1}$.

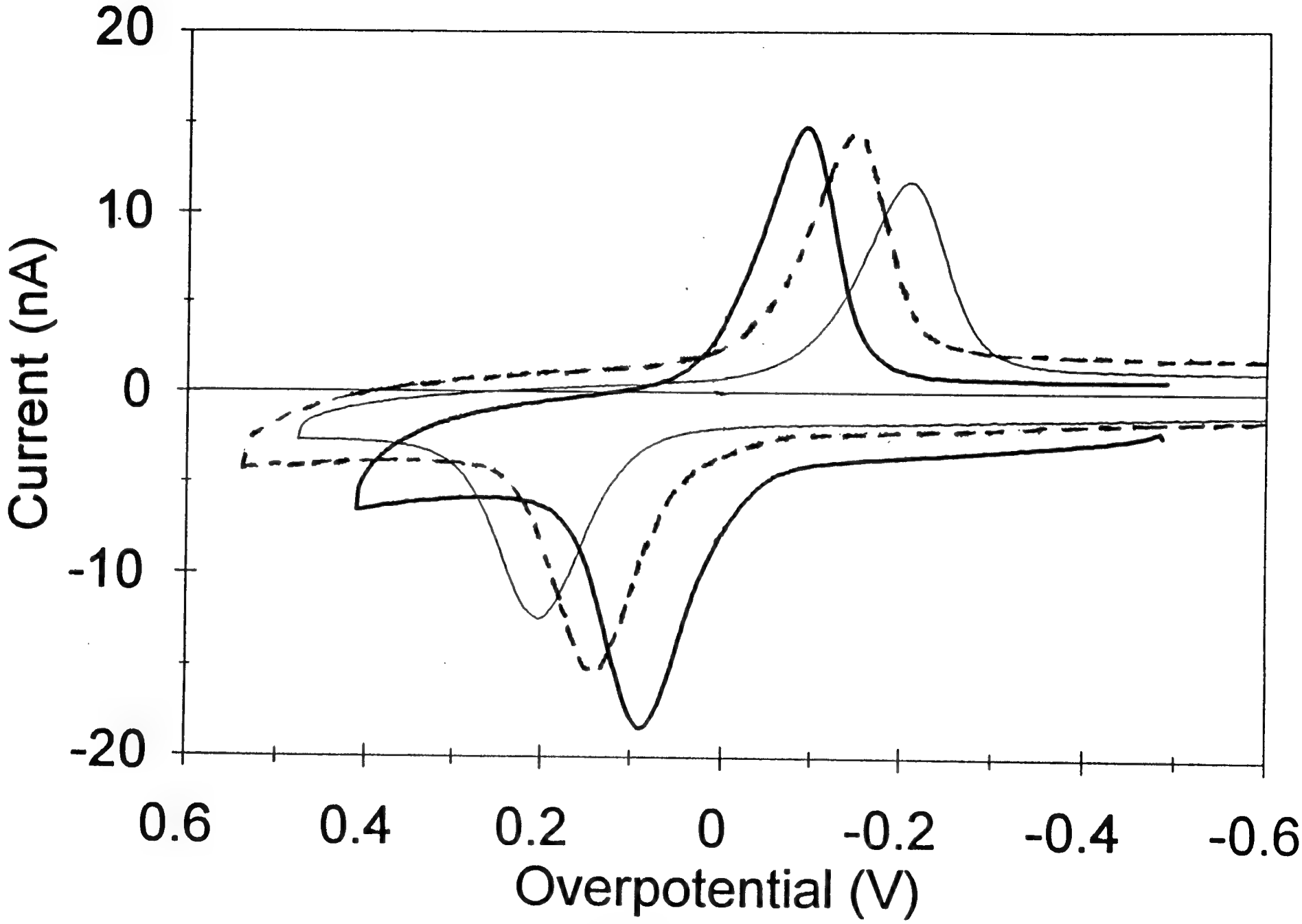
20
10
0
-10
-20
Current (nA)
0.6
0.4
0.2
0
-0.2
-0.4
-0.6
Overpotential (V)

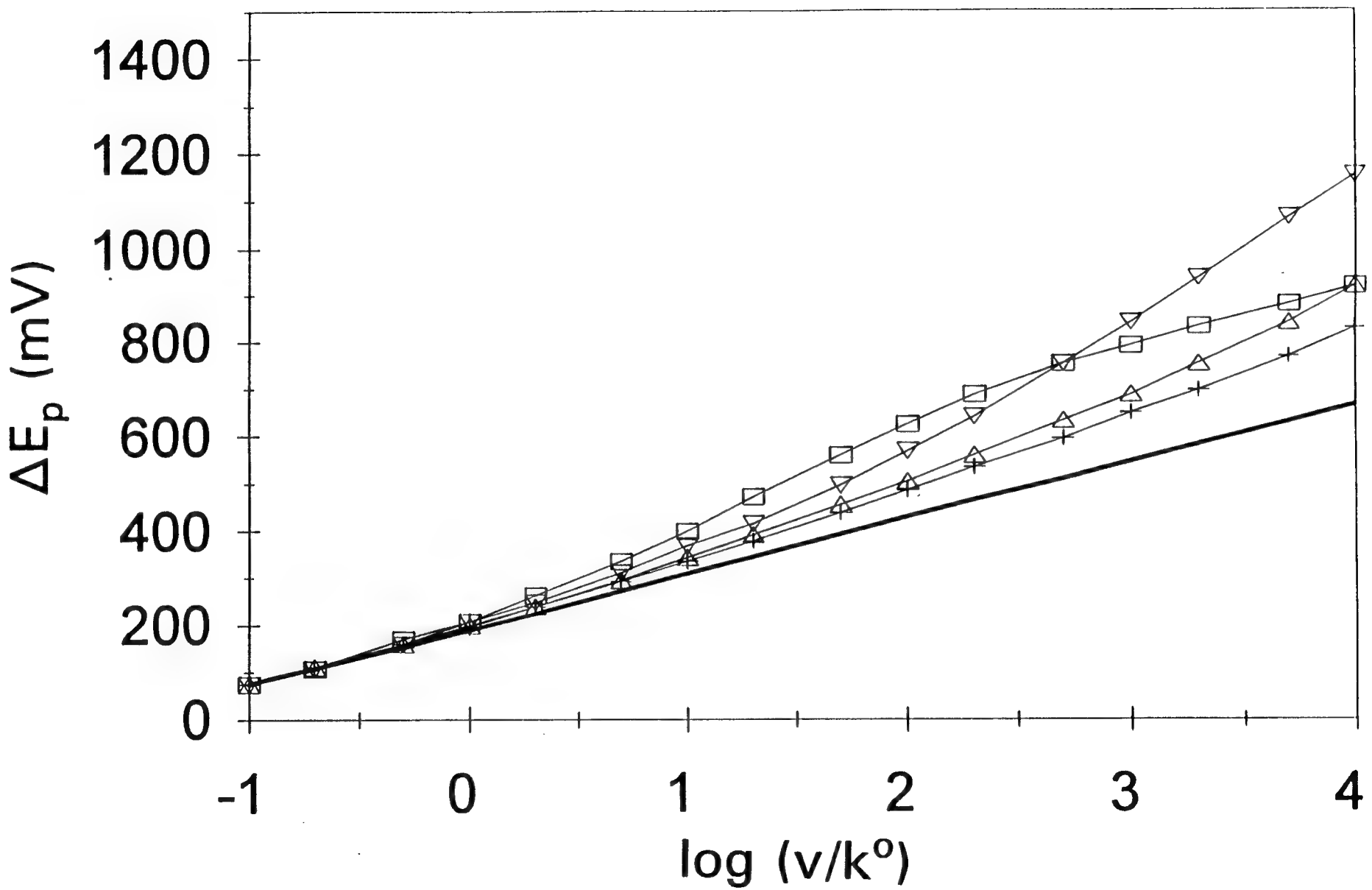
1400
1200
1000
800
600
400
200
0
ΔEp (mV)
-1
0
1
2
3
4
log (v/k°)

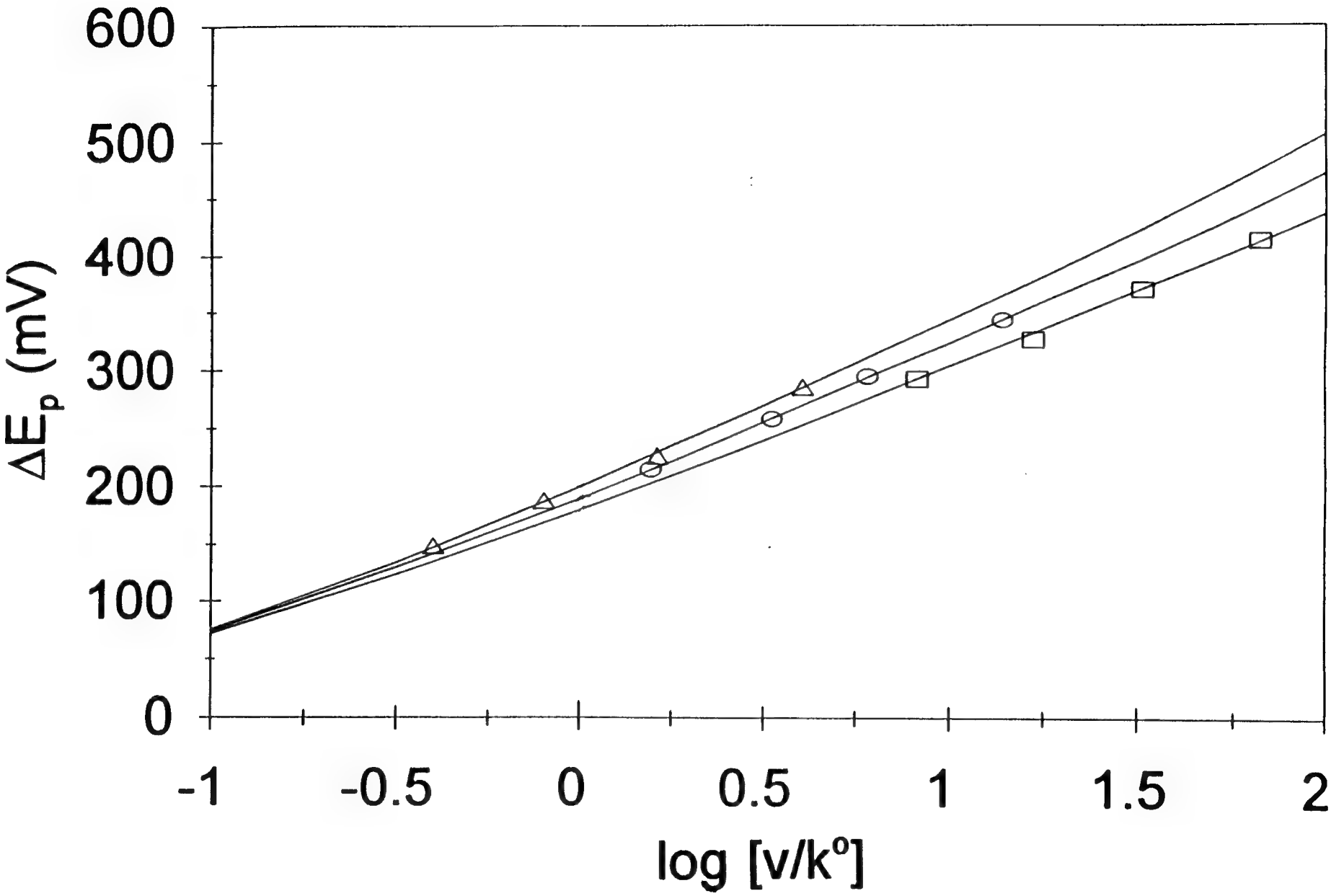
600
500
400
300
200
100
0
ΔE_p (mV)
-1
-0.5
0
0.5
1
1.5
2
log [v/k°]

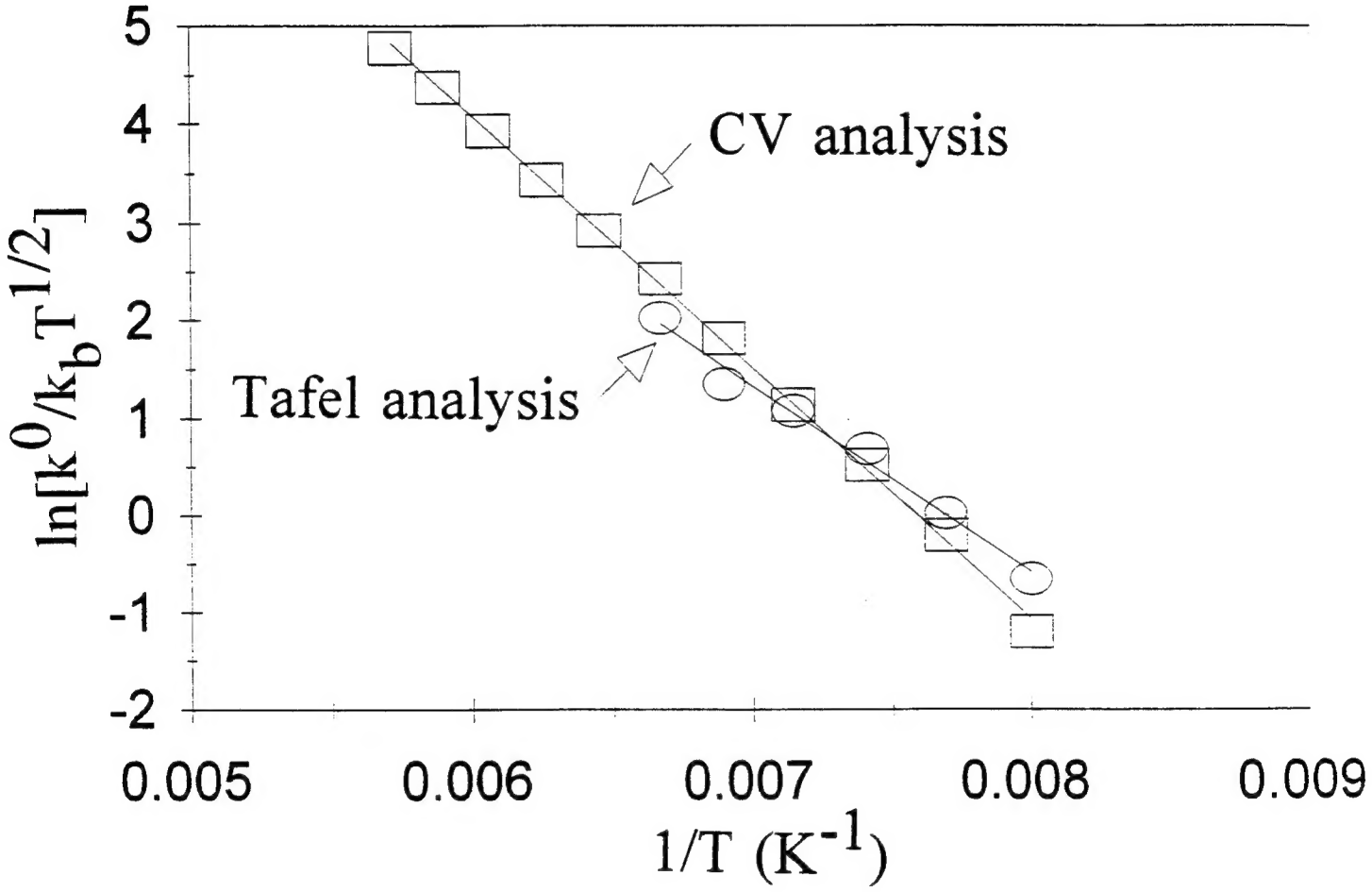
5
4
3
2
1
0
-1
-2
0.005
0.006
0.007
0.008
0.009
1/T (K-1)
ln[k0/kbT1/2]
CV analysis
Tafel analysis

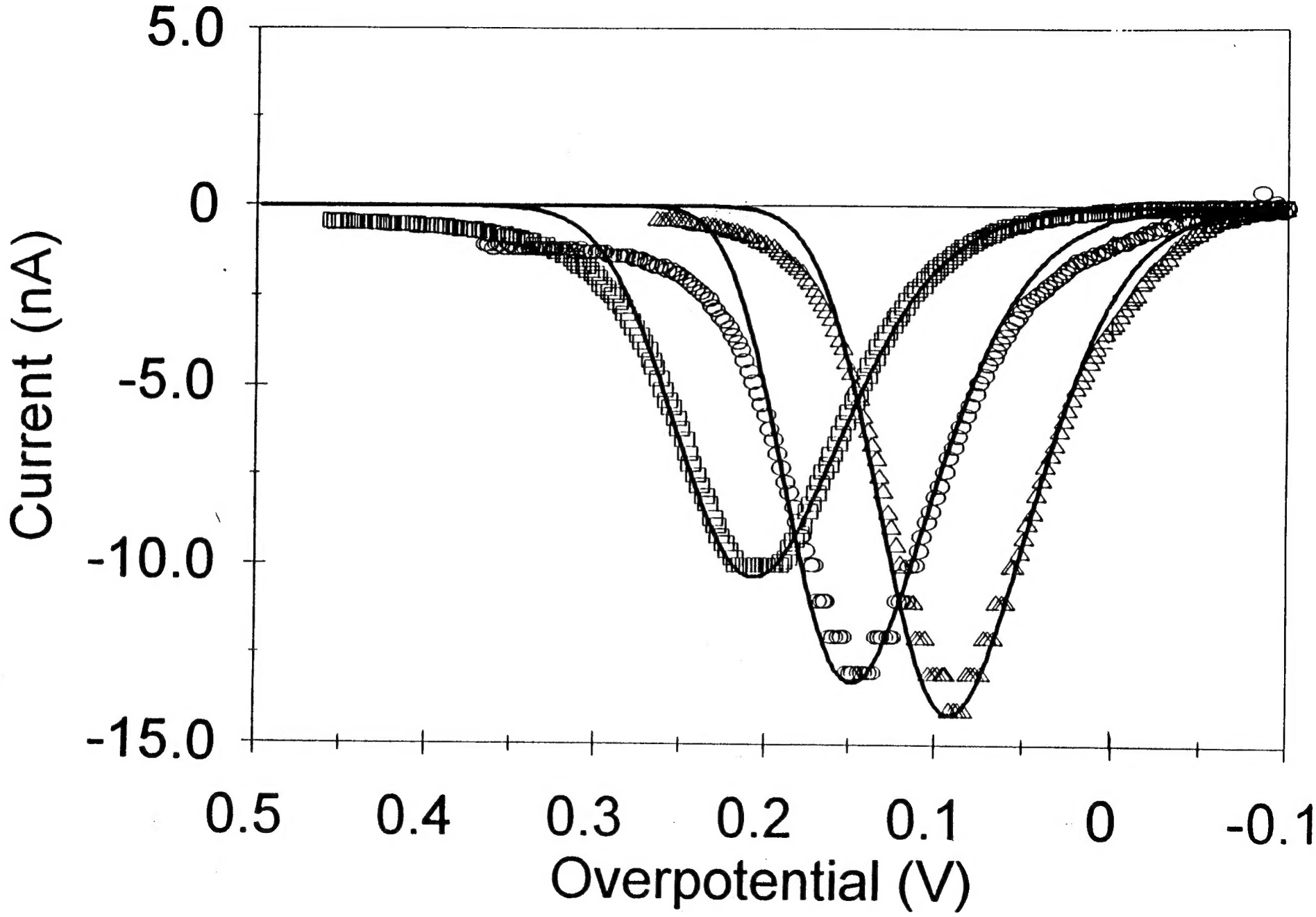
5.0
0
-5.0
-10.0
-15.0
Current (nA)
0.5
0.4
0.3
0.2
0.1
0
-0.1
Overpotential (V)

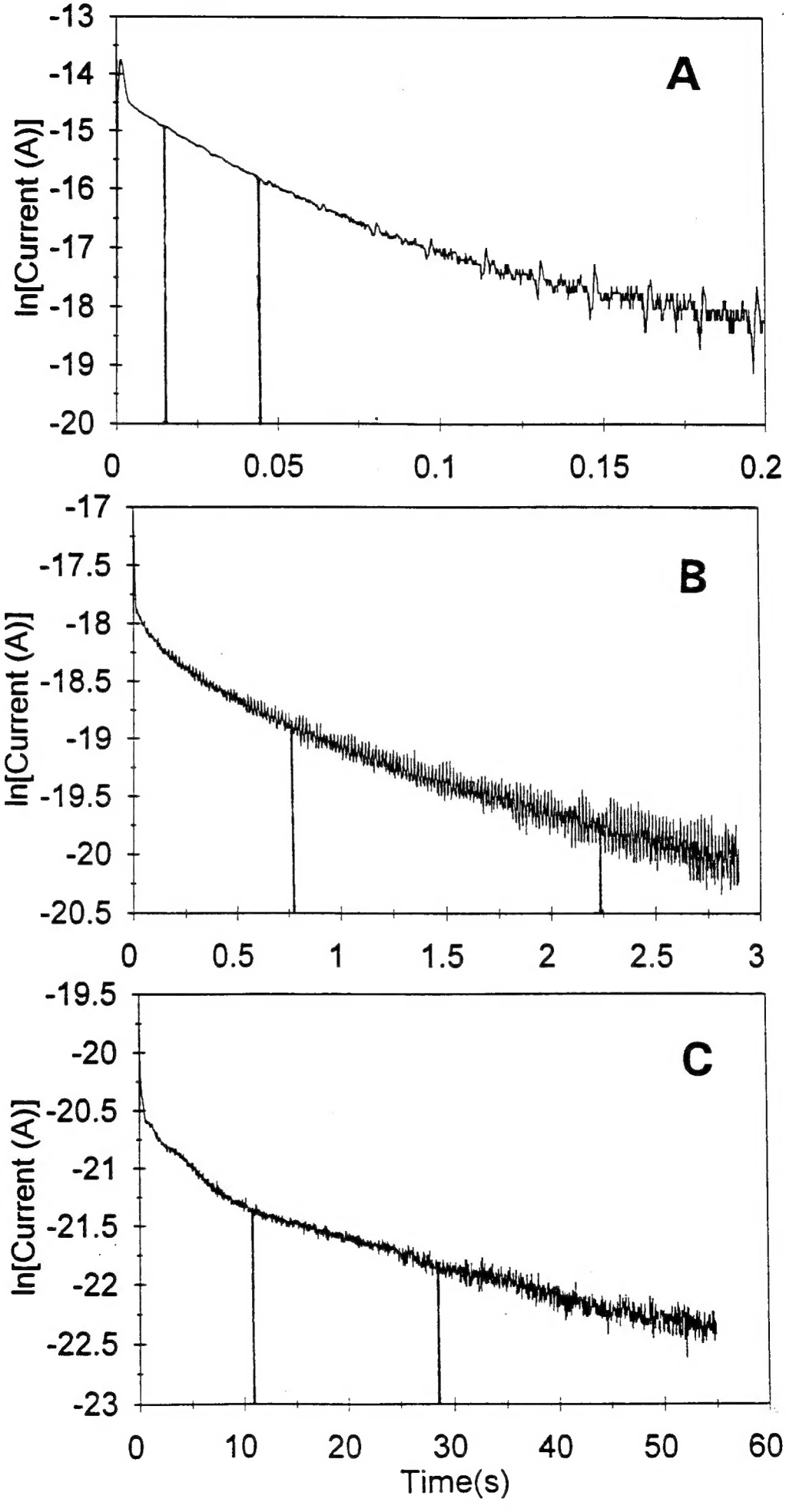
A
B
C
ln[Current (A)]
Time(s)
-13
-14
-15
-16
-17
-18
-19
-20
0
0.05
0.1
0.15
0.2
-17
-17.5
-18
-18.5
-19
-19.5
-20
-20.5
0
0.5
1
1.5
2
2.5
3
-19.5
-20
-20.5
-21
-21.5
-22
-22.5
-23
0
10
20
30
40
50
60

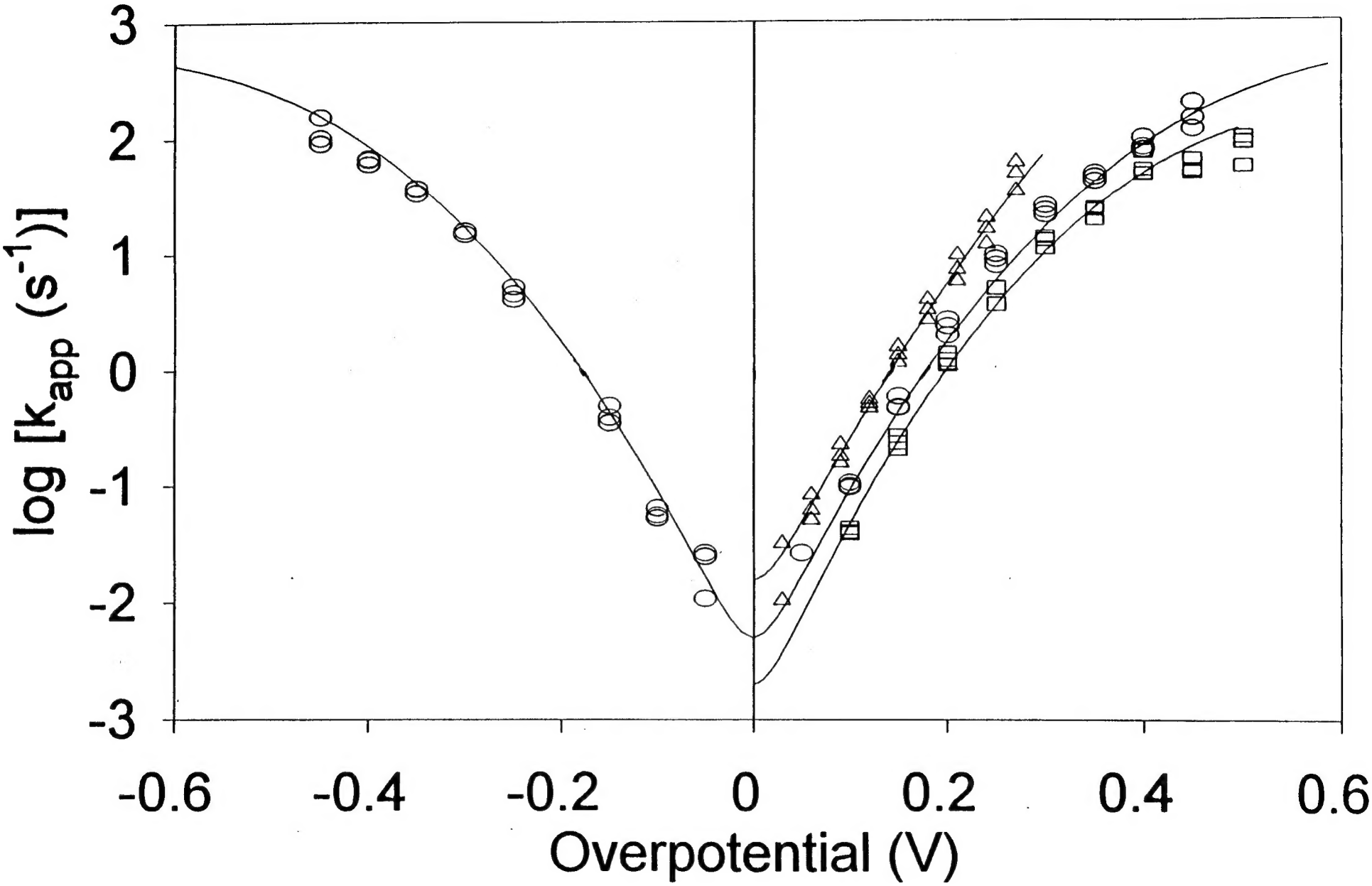
3
2
1
0
-1
-2
-3
log [k_{app} (s^{-1})]
-0.6
-0.4
-0.2
0
0.2
0.4
0.6
Overpotential (V)